

Tuning magnetic properties with crystal engineering in a family of coordination polymers based on Ni(II) sulphates

Anabel B. González Guillén^a, Piotr Konieczny^{b}, Katarzyna Luberda-Durnaś^c, Marcin
Oszajca^a, Marcin Koziel^{a*}, Wiesław Łasocha^{ad}.*

^a Faculty of Chemistry, Jagiellonian University, Gronostajowa 2, 30-387 Krakow, Poland

^b Institute of Nuclear Physics Polish Academy of Sciences, Radzikowskiego 152, PL-31342
Krakow, Poland

^c Institute of Geological Science Polish Academy of Sciences, Senacka 1, 31-002 Krakow,
Poland

^d Jerzy Haber Institute of Catalysis and Surface Chemistry Polish Academy of Sciences,
Niezapominajek 8, 30-239 Krakow

Table S1. Synthesis proportions.

Material	Formula	NiSO ₄ ·4H ₂ O	Amine
1	C ₁₂ H ₁₆ N ₄ NiO ₄ S	10 mmol (2.26g)	1,2-phenylenediamine 25 mmol (2.70g)
2	C ₁₂ H ₁₆ N ₄ NiO ₄ S	10 mmol (2.26g)	1,3-phenylenediamine 25 mmol (2.70g)
3	C ₆ H ₆ N ₂ NiSO ₄	10 mmol (2.26g)	1,4-phenylenediamine 11.5 mmol (1.24g)

Scanning electron microscopy

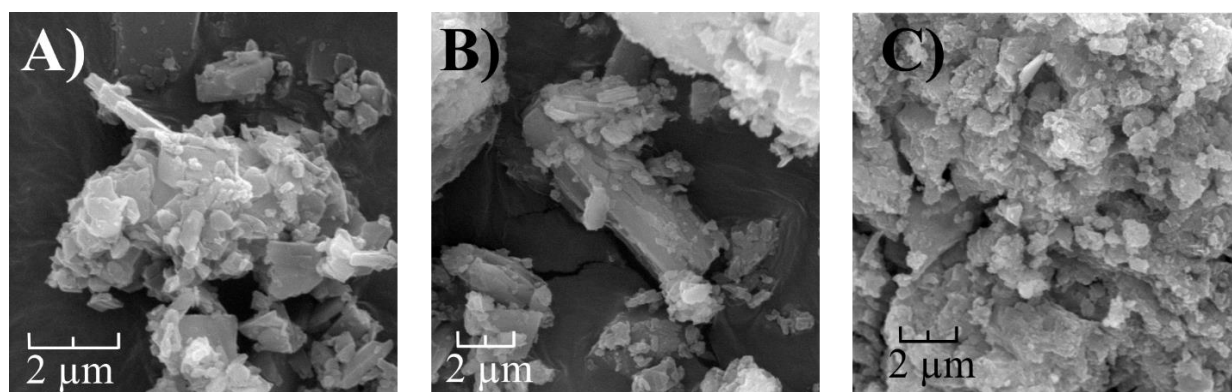


Figure S1: SEM images of A) **1**, B) **2** and C) **3**.

Scanning electron microscopy images (Figure S1) reveal some similarities between the samples of **1** and **2**. There is a tendency for these substances to form plate-like crystals with a wide range of sizes. The visible crystallites are larger than ca 0.3 μm with a majority larger than 0.5 μm. Bigger and better-developed crystals are also observed. In the case of **3** the observed morphology exhibits much finer granularity. Larger crystals are covered with small irregular crystallites-

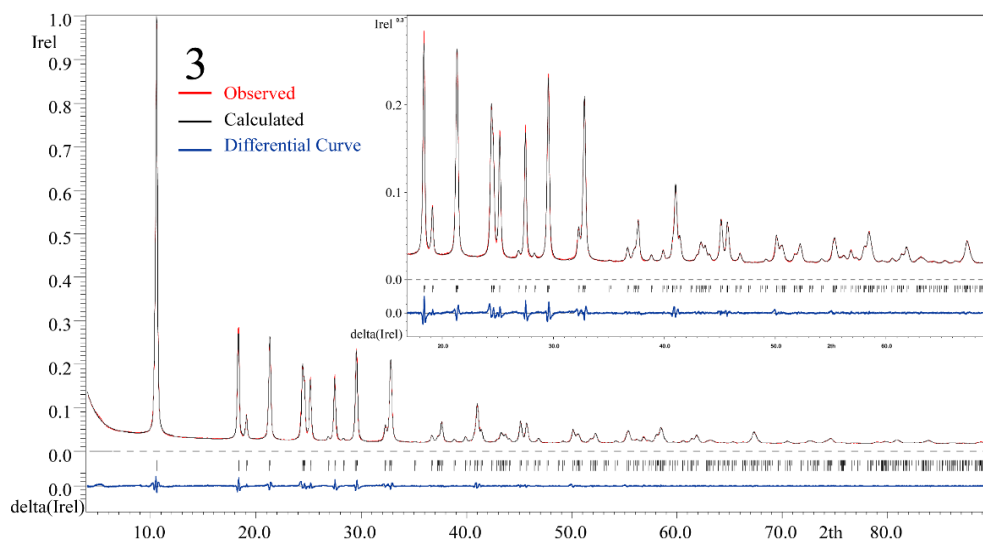
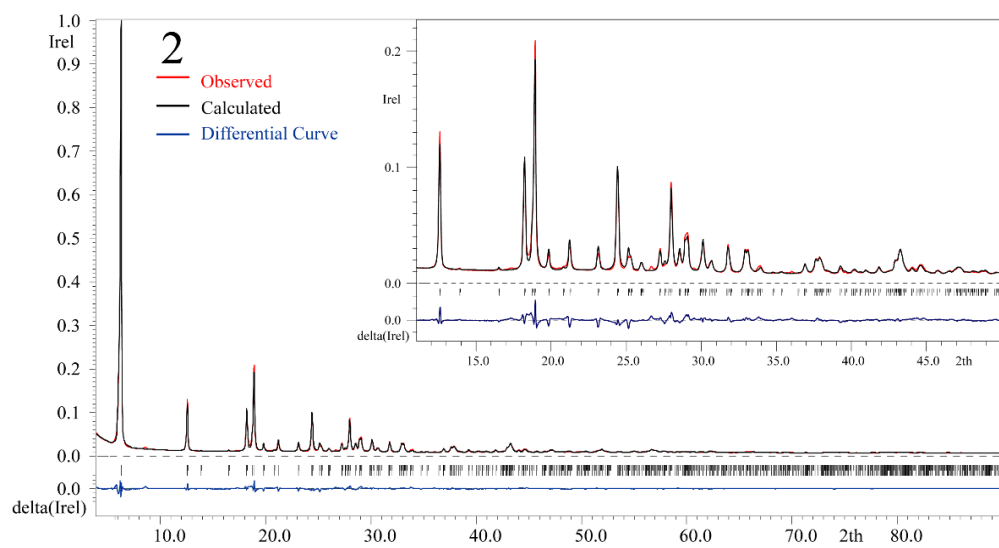
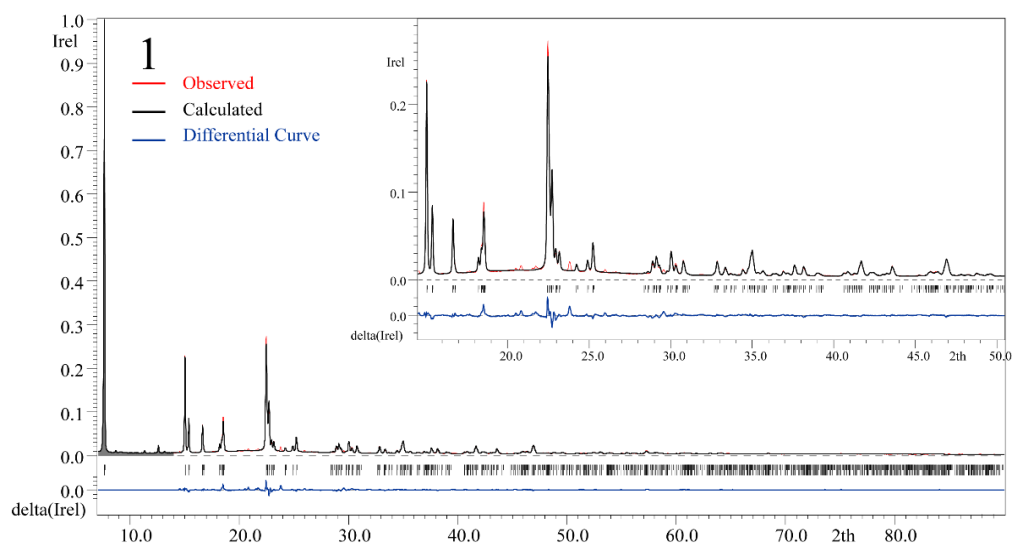


Figure S2. Rietveld plots for compounds **1**, **2** and **3**.

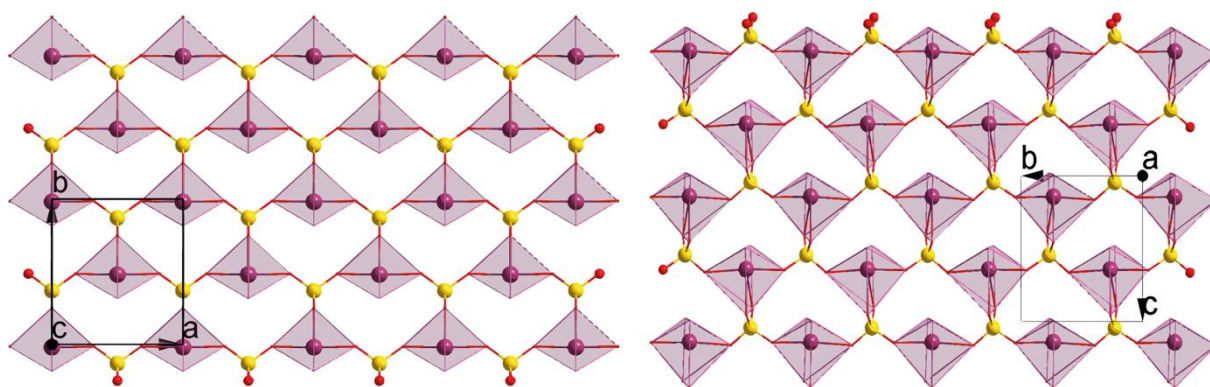


Figure S3. Inorganic layer of **2** (right) and **3** (left).

Thermal stability of hybrid materials. The general pattern of the thermal behaviour of hybrid compounds seems to be strongly correlated with the structure dimensionality of the compounds, however it is also influenced by the used atmosphere. With exception of one case, **3**(3D) in nitrogen, a multi-step thermal decomposition is observed. Based on the mass loss calculations for the process, the decomposition steps could be described as three main stages: (1) Removal of water adsorbed on the surface of the material and removal of amine from the framework, (2) removal of the amine residue with the start of sulphate decomposition (SO_x/O_2) and (3) further sulphate decomposition SO_x/O_2 . Depending on the atmosphere, the observed temperature of individual steps differ. In case of **3** in nitrogen, the first and second step occur simultaneously, thus only two-steps thermal decomposition can be observed. All of above stages for all samples are clearly indicated in Figures S4-S12.

Table S2. Steps of the thermal decompositions in air.

Weight Loss [wt%]	Decomposition Product	Temperature range [°C]	Final Product	Total mass released
1				
28.5	Water and amine	50–360	NiO	~80.2% (calc.80 %)
43.6	Amine + SO_x/O_2^*	360–625		
8.1	SO_x/O_2	625–800		
2				
39.2	Water and amine	50–440	NiO	~79.7%

37.2	Amine + SO _x /O ₂	440–470		(calc. 80%)
3.3	SO _x /O ₂	470–800		
3				
24.5	Water and amine	50–440		
			NiO	~73.3%
45.5	Amine + SO _x /O ₂	440–490		(calc. 72%)
3.3	SO _x /O ₂	490–800		
* SO _x : products of sulfate decomposition: SO ₃ , SO ₂ + O ₂ , etc				

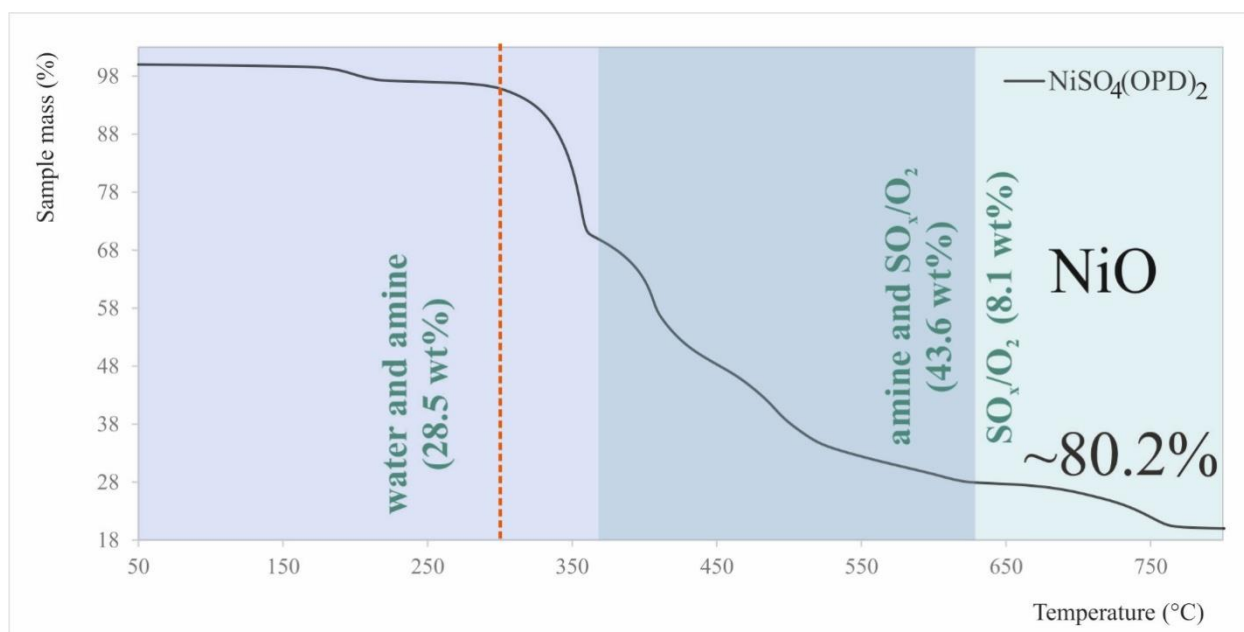


Figure S4. TG curves representing ramp experiments of sample **1** in air; ramp rate 10°C/min. The orange dashed line represents the boundary between rapid and slow amine removing. The three steps of thermal decompositions are shown by colours; light blue – water and amine removing, dark blue- amine and SO_x/O₂ removing; green –SO_x/O₂ removing.

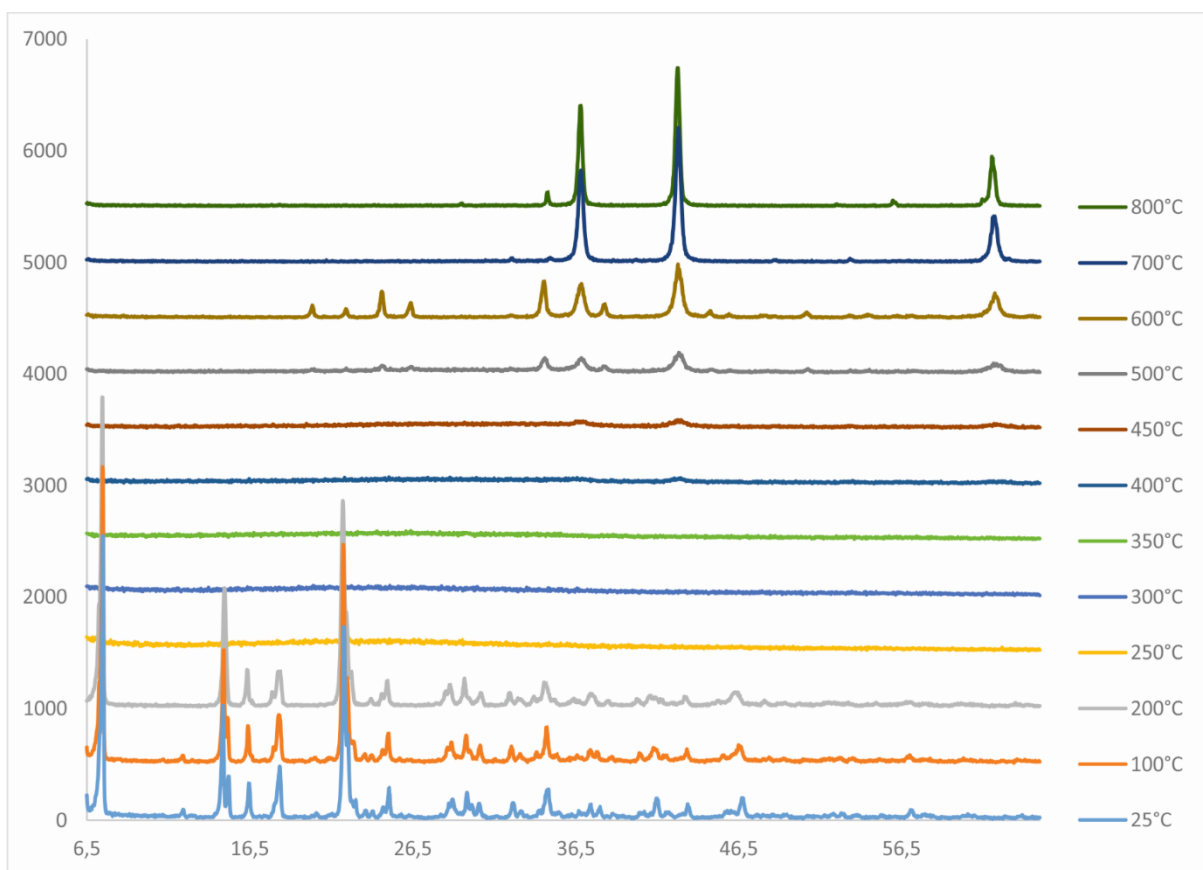


Figure S5. XRD patterns in different temperature of **1** in air; ramp rate 10°C/min. **1** from 25°C – 200°C; amorphous from 250°C – 450°C; NiO (01-089-3080), Ni₂S₃ (04-018-6476) and Ni(SO₄) from 500°C-600 °C; NiO (01-078-4370) at 700°C; and NiO (04-013-0888 and 01-078-4367) at 800°C.

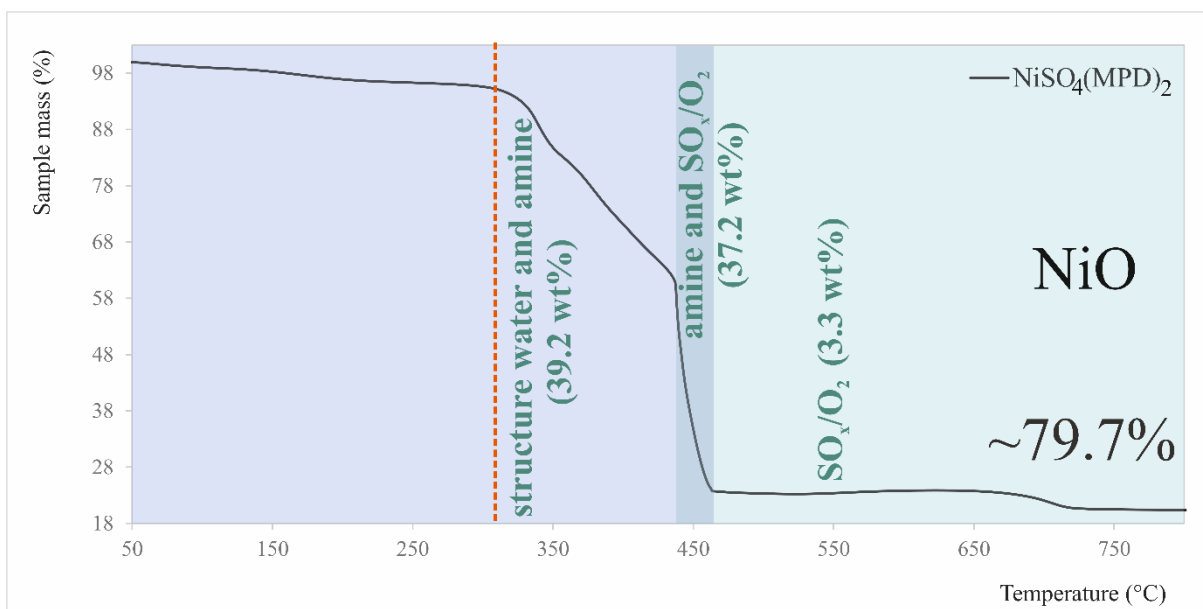


Figure S6. TG curves representing ramp experiments of sample **2** in air; ramp rate 10°C/min. The orange dashed line represents the boundary between rapid and slow amine removing. The three steps of thermal decompositions are shown by colours; light blue – water and amine removing, dark blue- amine and SO_x/O₂ removing; green –SO_x/O₂ removing.

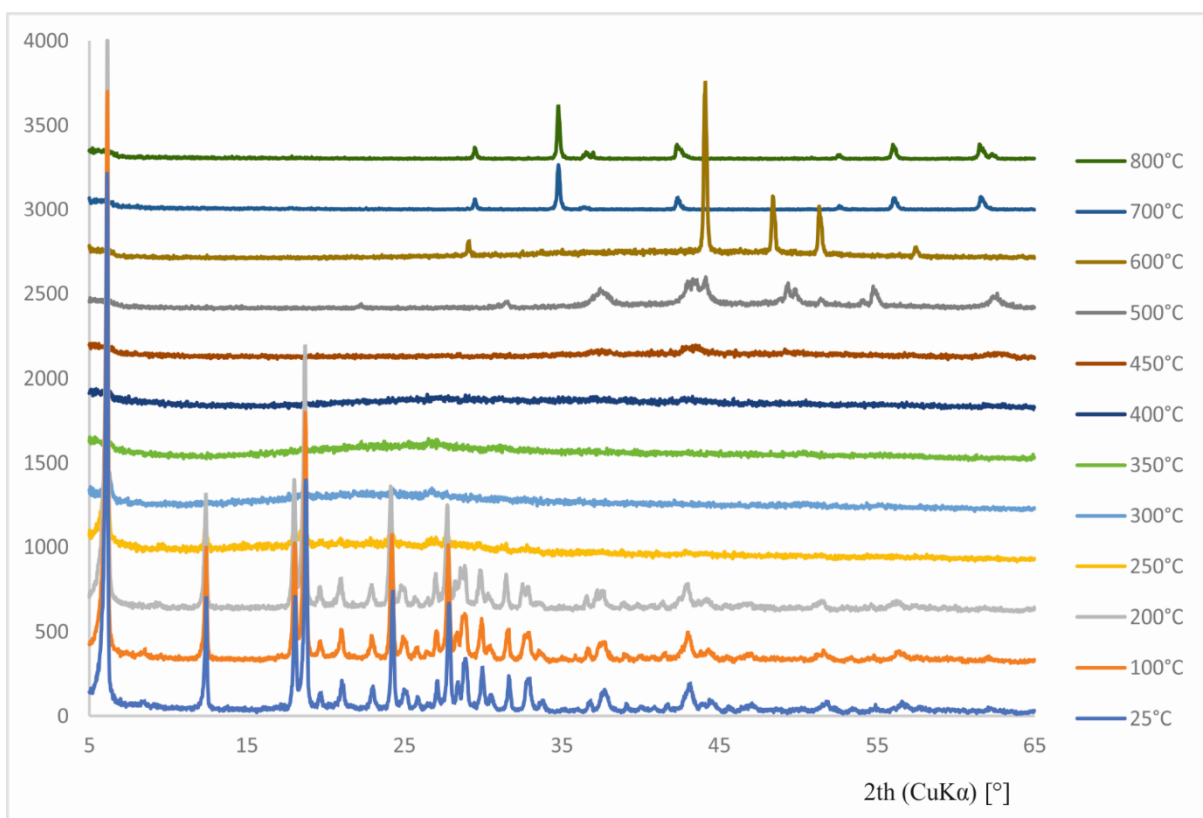


Figure S7. XRD patterns in different temperature of **2** in air; ramp rate 10°C/min. **2** from 25°C – 200°C; NiS (04-002-7227), Ni (04-016-4592), and Ni_{1.5}S (04-012-6387) at 500 °C; NiO (01-071-4750) and Ni at 600 °C; and NiO (01-078-4367 and 01-089-3080) at 800°C.

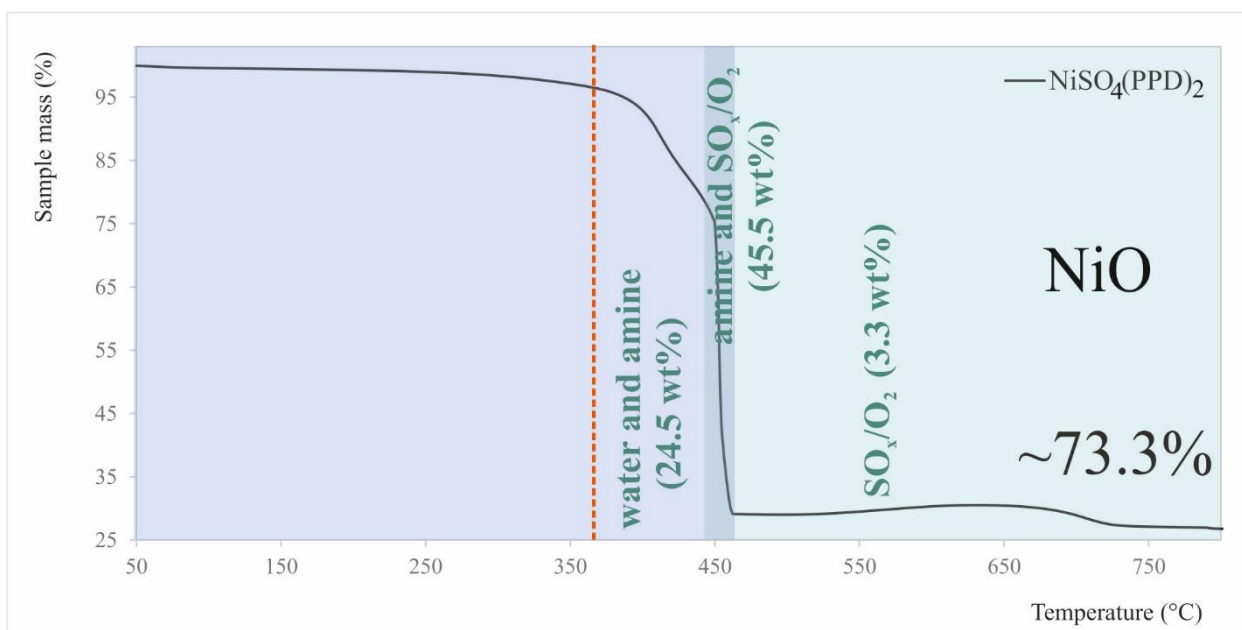


Figure S8. TG curves representing ramp experiments of sample **3** in air; ramp rate 10°C/min. The orange dashed line represents the boundary between rapid and slow amine removing. The three steps of thermal decompositions are shown by colours; light blue – water and amine removing, dark blue- amine and SO_x/O₂ removing; green –SO_x/O₂ removing.

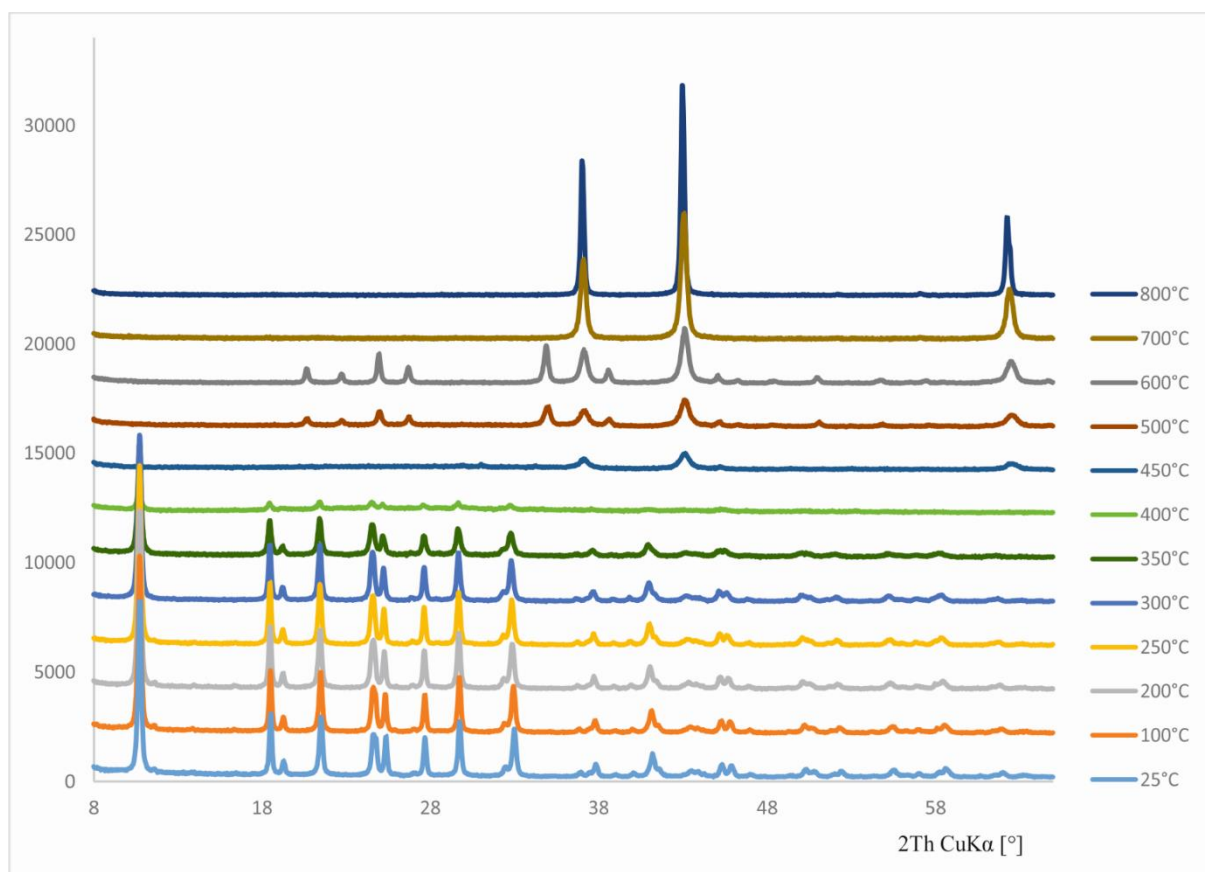


Figure S9. XRD patterns in different temperature of **3** in air; ramp rate 10°C/min. **3** from 25 °C to 350 °C; NiSO₄ (04-009-5720) from 500 °C to 600 °C; NiO (01-078-4376) from 700 °C to 800 °C.

Table S3. Steps of the thermal decompositions in nitrogen.

Weight Loss [wt%]	Decomposition Product	Temperature range [°C]	Final Product	Total mass released
1				
44.7	Water and amine	50–380	Ni ₃ S ₂	~77.2% (calc.78 %)
14.8	Amine + SO _x /O ₂ *	380–460		
17.7	SO _x /O ₂	460–800		
2				
45.8	Water and amine	50–380	Ni ₃ S ₂	~74.0% (calc. 78%)
11.5	Amine + SO _x /O ₂	380–460		
16.7	SO _x /O ₂	460–800		
3				

55.1	Water, amine and SO _x /O ₂	50–540	Ni ₄ S ₃ and Ni	~61.2%
6.1	SO _x /O ₂	540–800		(calc. 71%)
* SO _x : products of sulfate decomposition: SO ₃ , SO ₂ + O ₂ , etc				

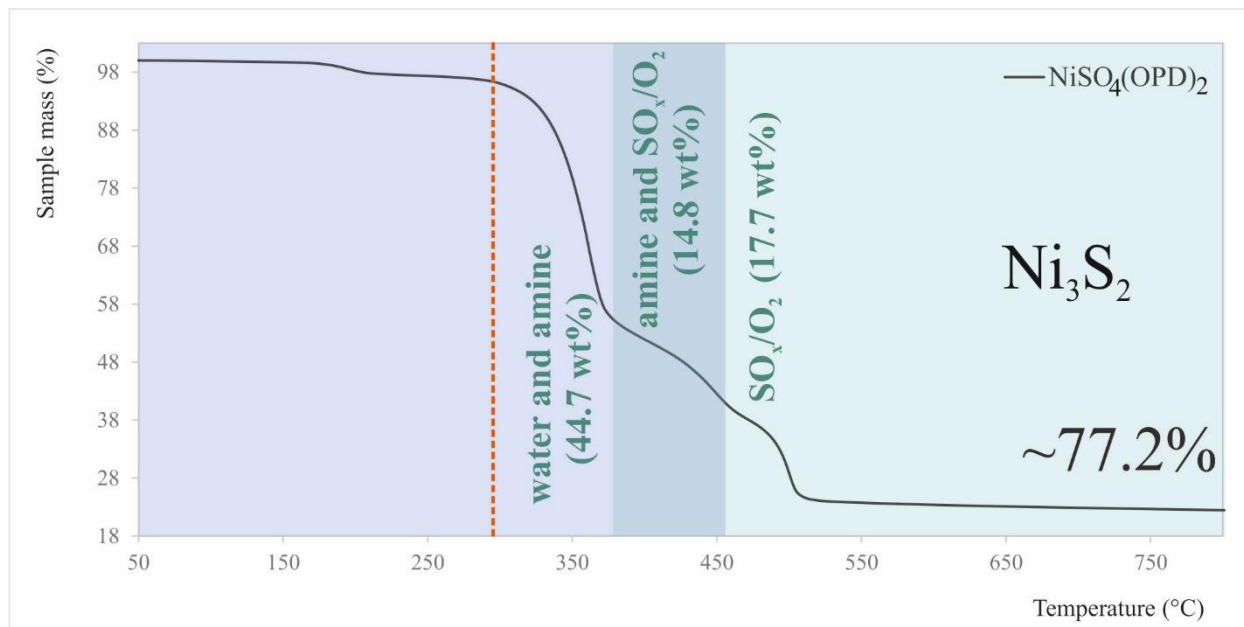


Figure S10. TG curves representing ramp experiments of sample **1** in nitrogen atmosphere; ramp rate 10°C/min. The orange dashed line represents the boundary between rapid and slow amine removing. The three steps of thermal decompositions are shown by colours; light blue – water and amine removing, dark blue- amine and SO_x/O₂ removing; green –SO_x/O₂ removing.

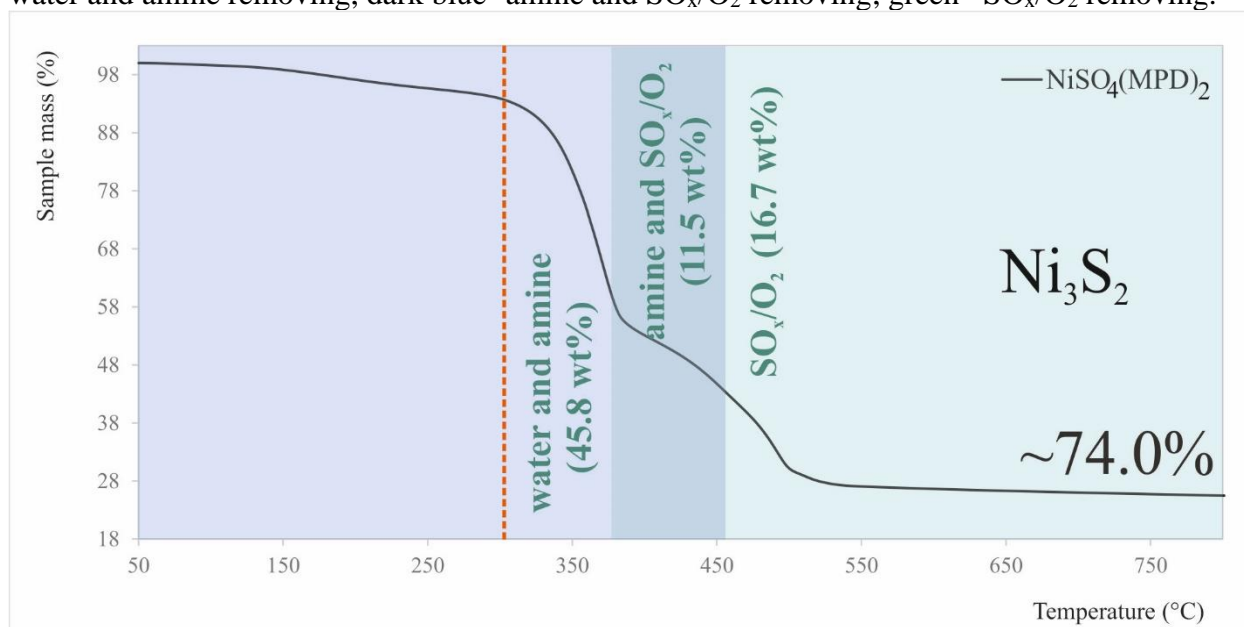


Figure S11. TG curves representing ramp experiments of **2** in nitrogen atmosphere; ramp rate 10°C/min. The orange dashed line represents the boundary between rapid and slow amine removing. The three steps of thermal decompositions are shown by colours; light blue – water and amine removing, dark blue- amine and SO_x/O₂ removing; green –SO_x/O₂ removing.

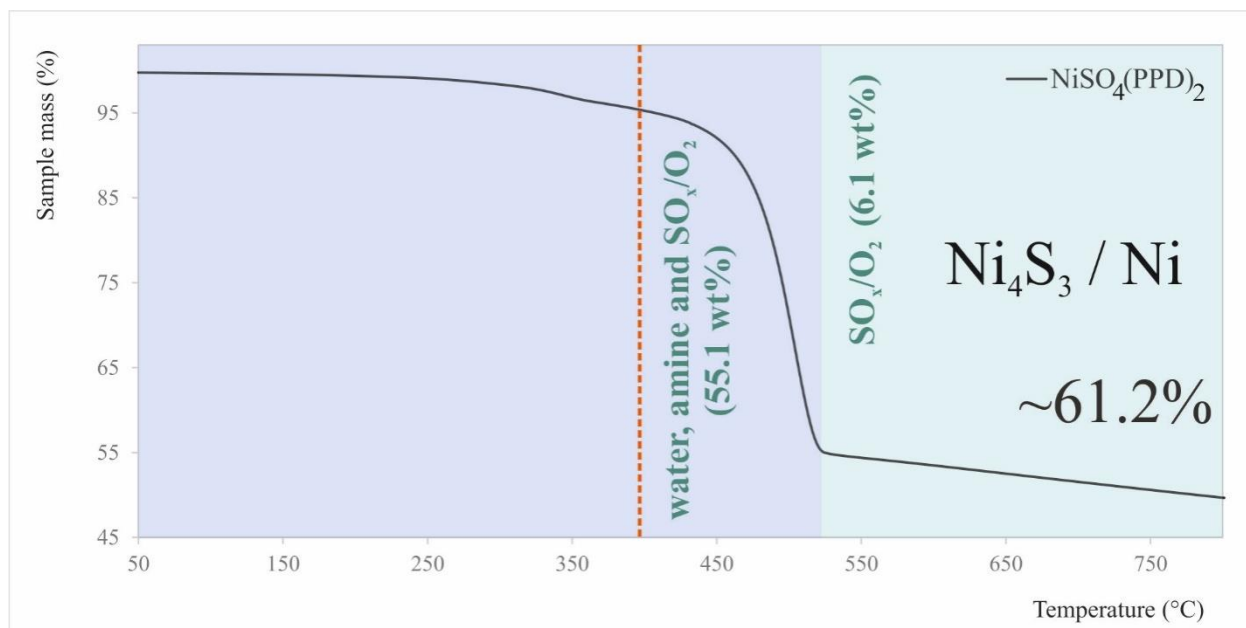


Figure S12. TG curves representing ramp experiments of **3** in nitrogen atmosphere; ramp rate 10°C/min. The orange dashed line represents the boundary between rapid and slow amine removing. The two steps of thermal decompositions are shown by colours; light blue – water, amine and SO_x/O₂ removing; green – sole SO_x/O₂ removing.

Magnetic studies

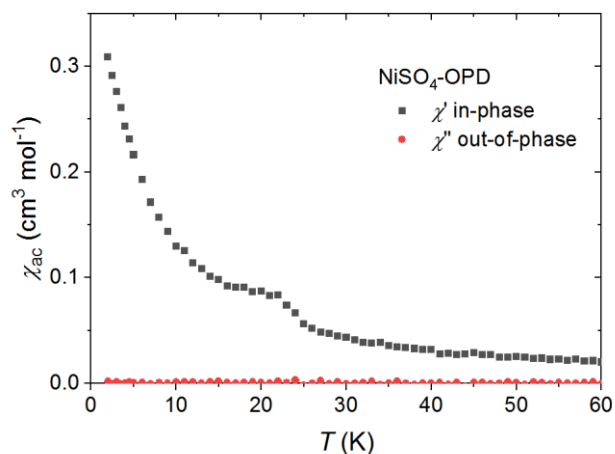


Figure S13. Temperature dependence of ac susceptibility of **1** for 100 Hz frequency. The black squares represent the in-phase component. The red circles stands for out-of-phase component.

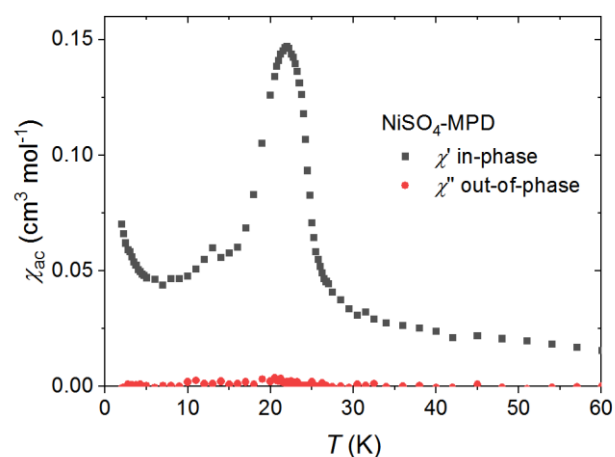


Figure S14. Temperature dependence of ac susceptibility of **2** for 100 Hz frequency. The black squares represent the in-phase component. The red circles stands for out-of-phase component.

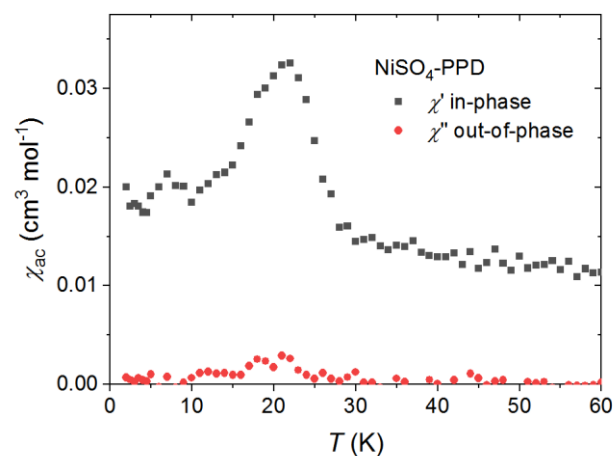


Figure S15. Temperature dependence of ac susceptibility of **3** for 100 Hz frequency. The black squares represent the in-phase component. The red circles stands for out-of-phase component.

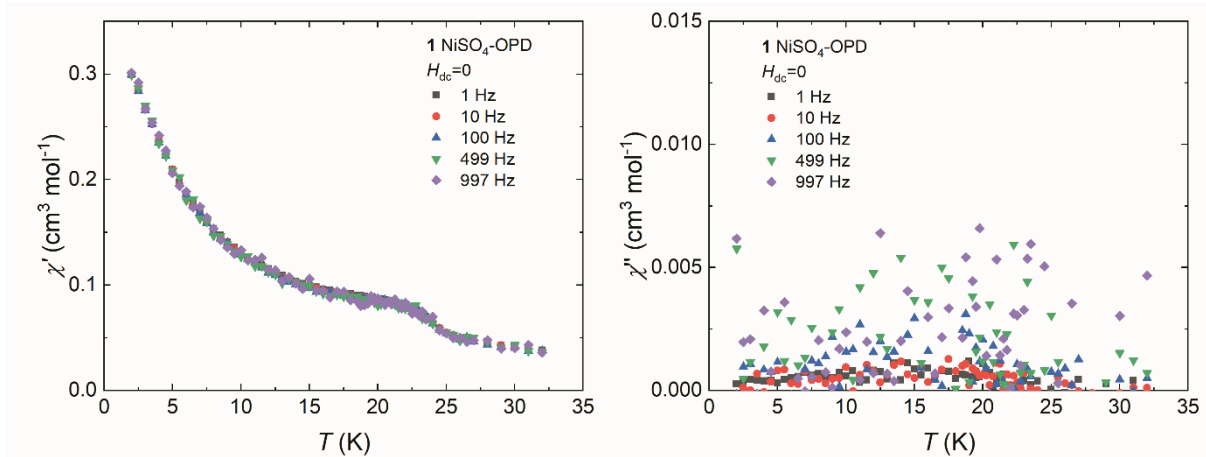


Figure S16. χ_{ac} vs. T data measured at frequency 1.0, 10, 100, 499 and 997 Hz for **1**. Left: in-phase component of χ_{ac} , right: out-of-phase component of χ_{ac} .

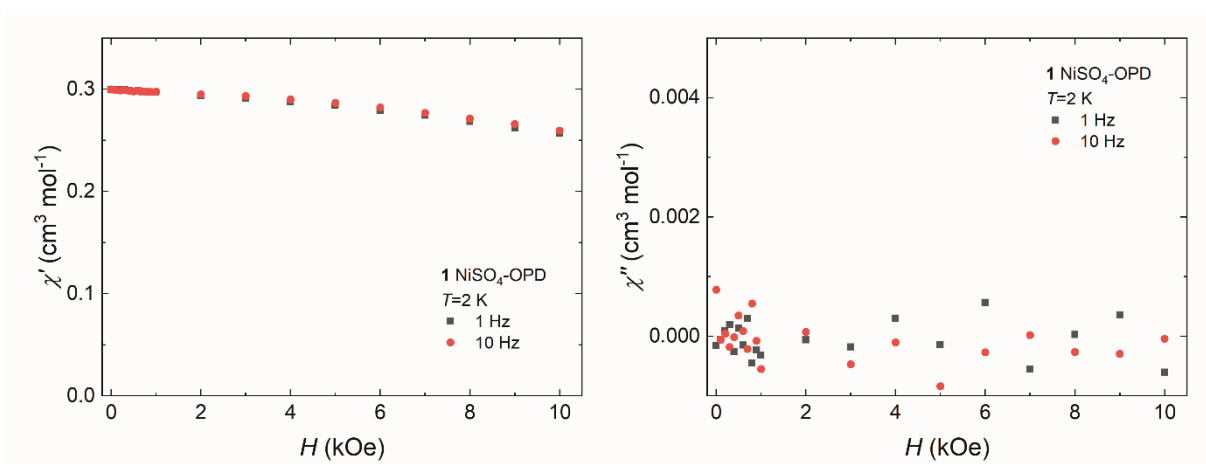


Figure S17. χ_{ac} vs. H_{dc} data measured at 2.0 K for frequency 1.0 and 10 Hz for **1**. Left: in-phase component of χ_{ac} , right: out-of-phase component of χ_{ac} .

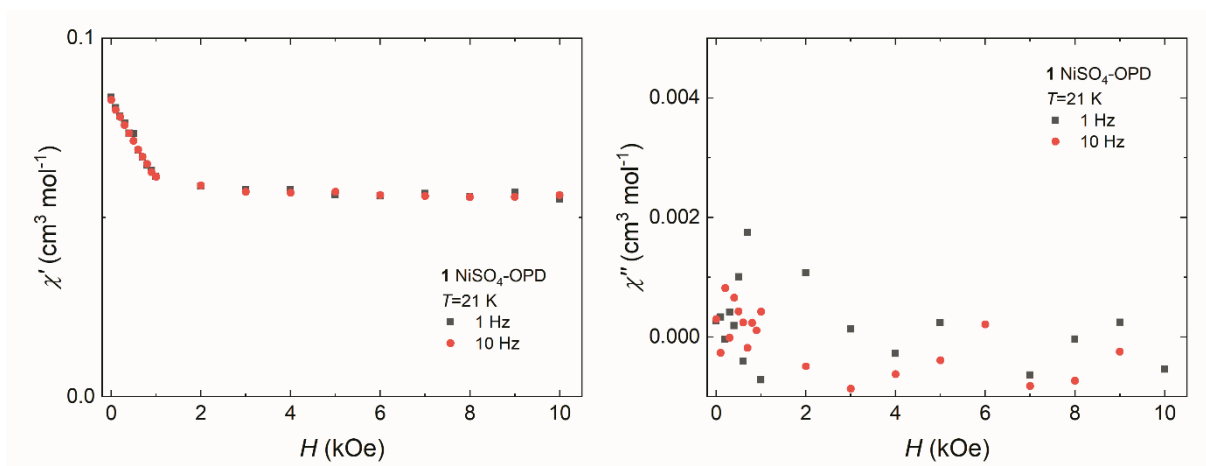


Figure S18. χ_{ac} vs. H_{dc} data measured at 21 K for frequency 1.0 and 10 Hz for **1**. Left: in-phase component of χ_{ac} , right: out-of-phase component of χ_{ac} .

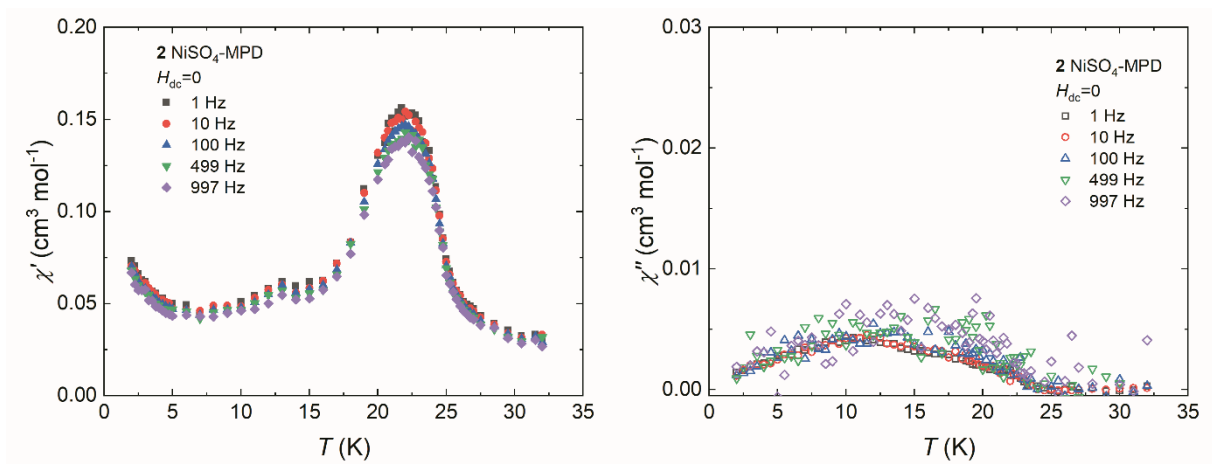


Figure S19. χ_{ac} vs. T data measured at frequency 1.0, 10, 100, 499 and 997 Hz for **2**. Left: in-phase component of χ_{ac} , right: out-of-phase component of χ_{ac} .

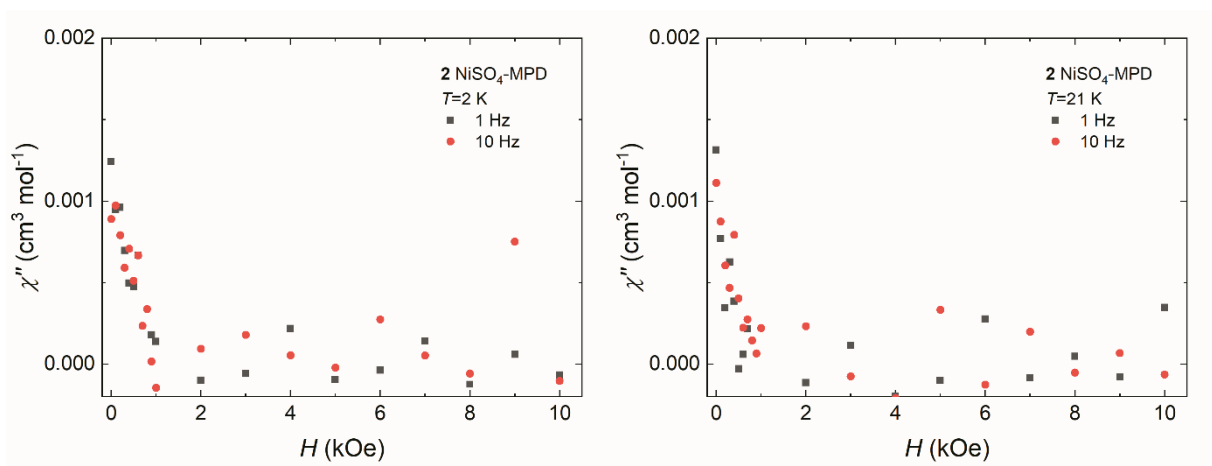


Figure S20. χ_{ac} vs. H_{dc} data measured at 2.0 K for frequency 1.0 and 10 Hz for **2**. Left: in-phase component of χ_{ac} , right: out-of-phase component of χ_{ac} .

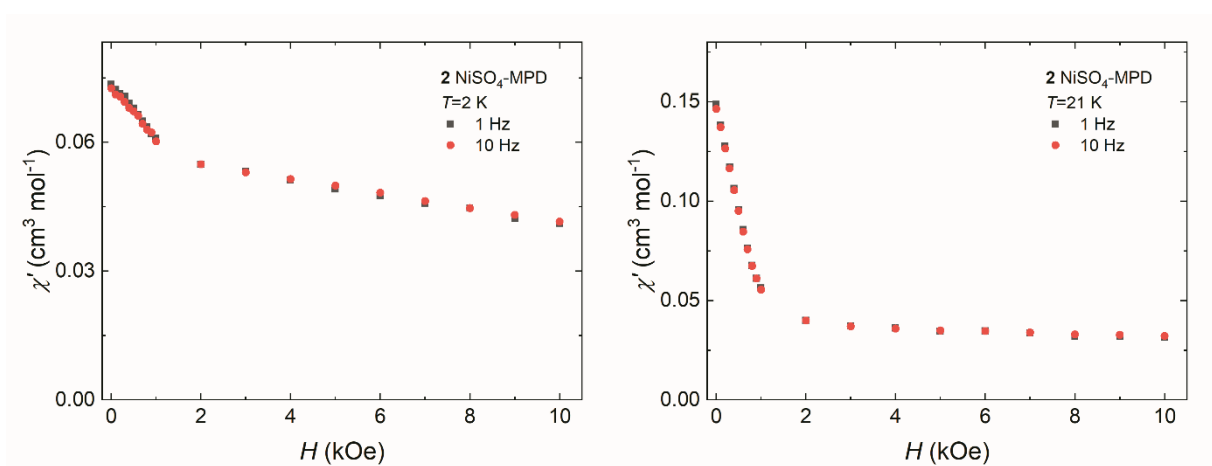


Figure S21. χ_{ac} vs. H_{dc} data measured at 21 K for frequency 1.0 and 10 Hz for **2**. Left: in-phase component of χ_{ac} , right: out-of-phase component of χ_{ac} .

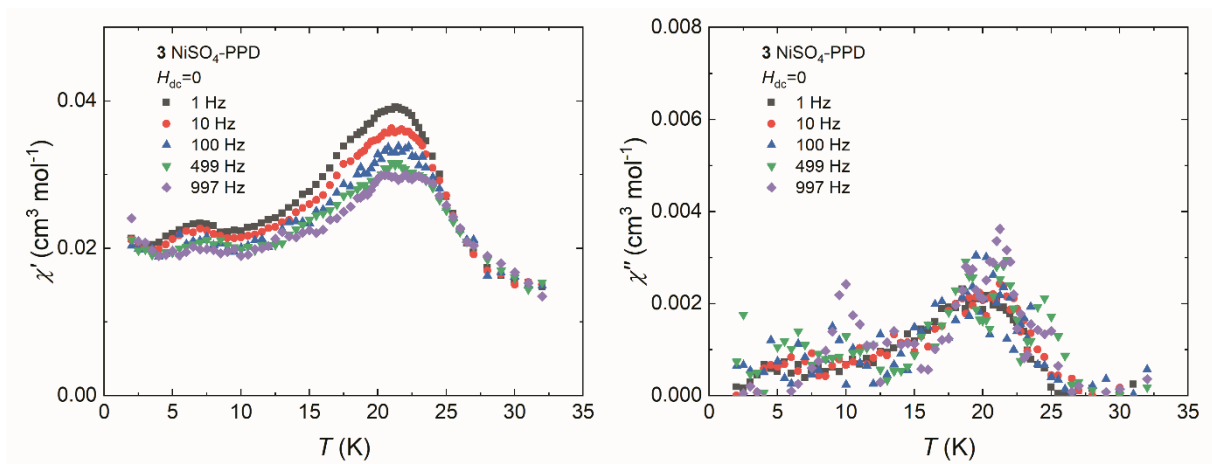


Figure S22. χ_{ac} vs. T data measured at frequency 1.0, 10, 100, 499 and 997 Hz for **3**. Left: in-phase component of χ_{ac} , right: out-of-phase component of χ_{ac} .

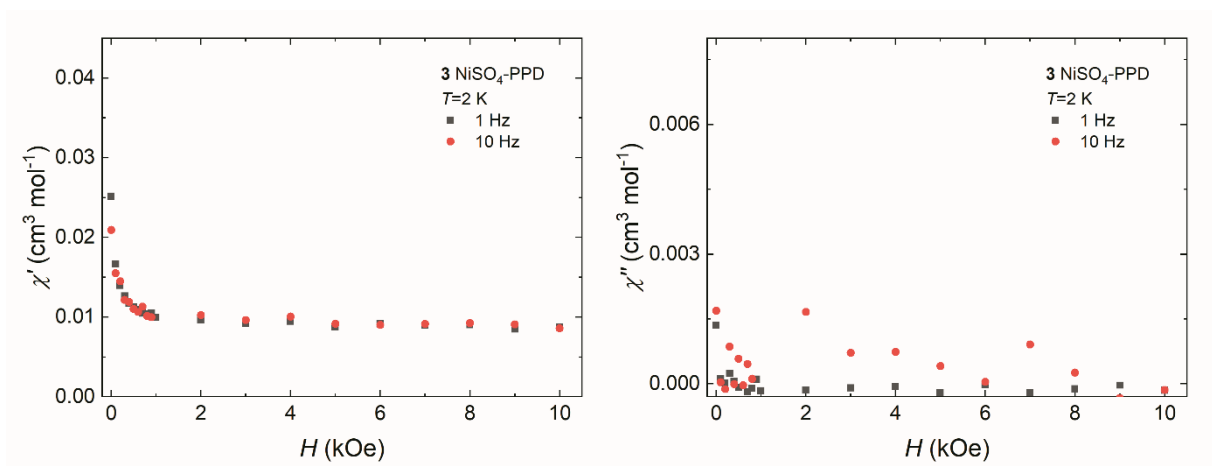


Figure S23. χ_{ac} vs. H_{dc} data measured at 2.0 K for frequency 1.0 and 10 Hz for **3**. Left: in-phase component of χ_{ac} , right: out-of-phase component of χ_{ac} .

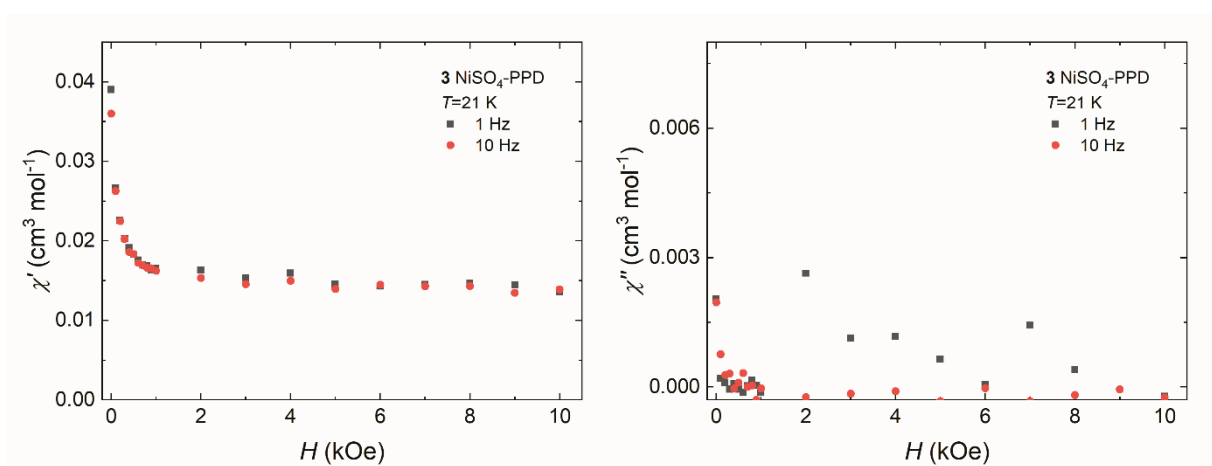


Figure S24. χ_{ac} vs. H_{dc} data measured at 21 K for frequency 1.0 and 10 Hz for **3**. Left: in-phase component of χ_{ac} , right: out-of-phase component of χ_{ac} .

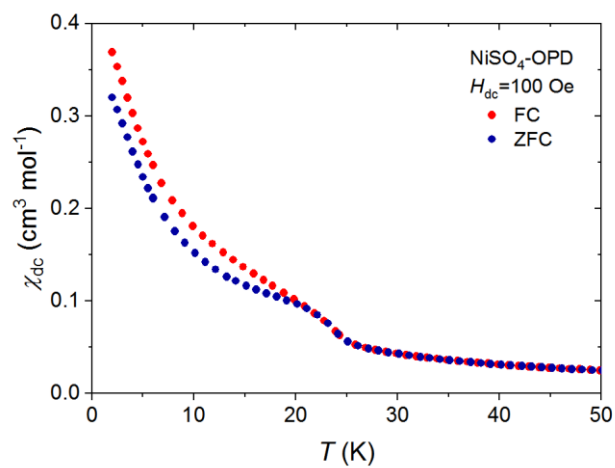


Figure S25. ZFC/FC susceptibility curves for **1**. The applied field was 100 Oe.

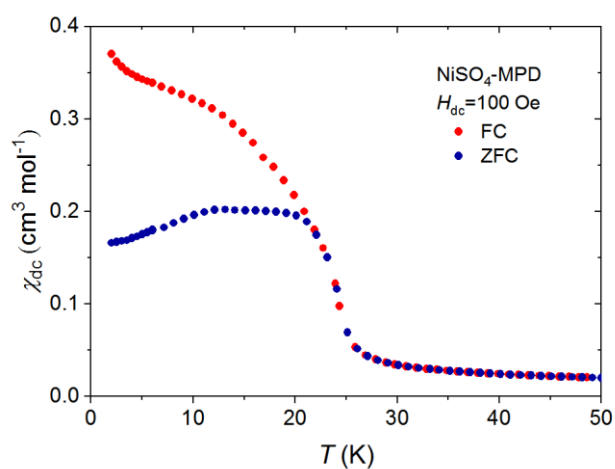


Figure S26. ZFC/FC susceptibility curves for **2**. The applied field was 100 Oe.

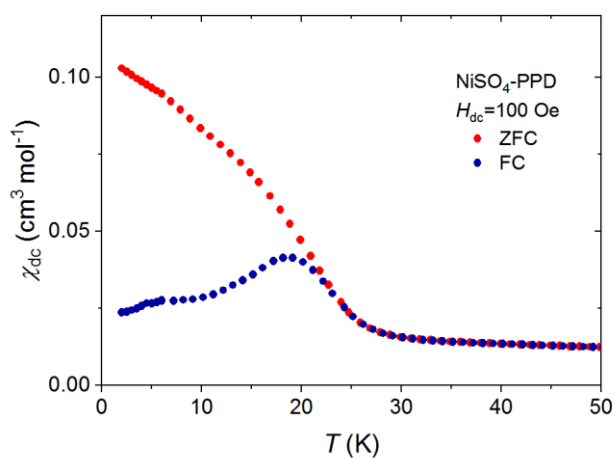


Figure S27. ZFC/FC susceptibility curves for **3**. The applied field was 100 Oe.

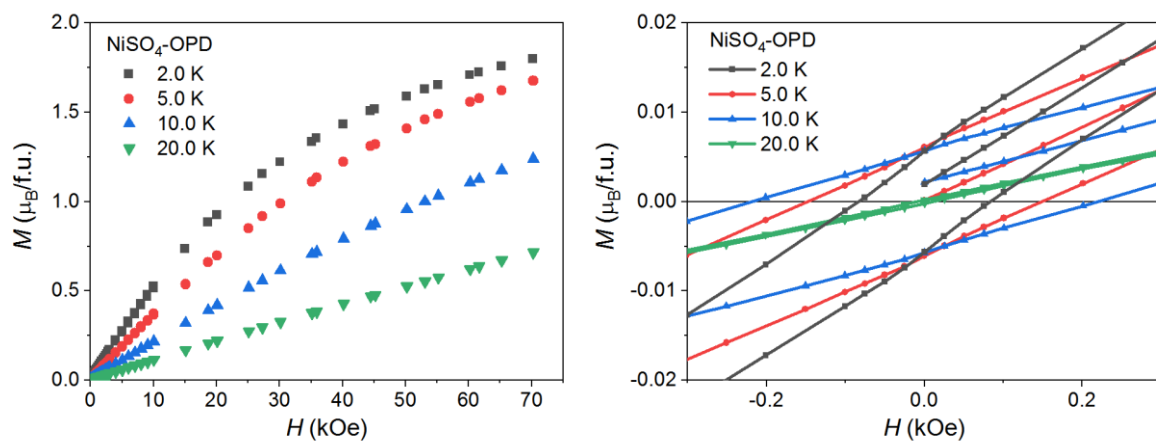


Figure S28. Field dependence of isothermal magnetization for **1** at 2.0 K (black squares), 5.0 K (red circles), 10.0 K (blue triangles) and 20.0 K (green triangles).

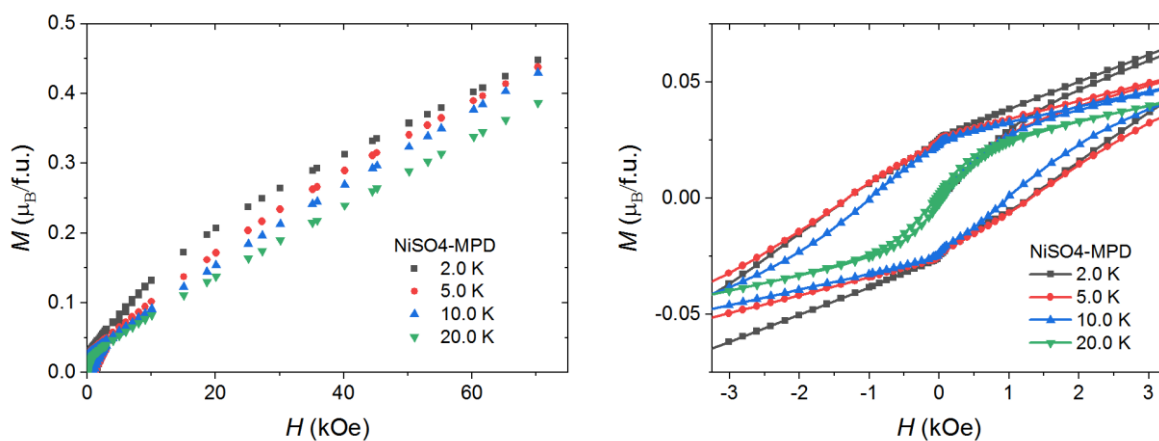


Figure S29. Field dependence of isothermal magnetization for **2** at 2.0 K (black squares), 5.0 K (red circles), 10.0 K (blue triangles) and 20.0 K (green triangles).

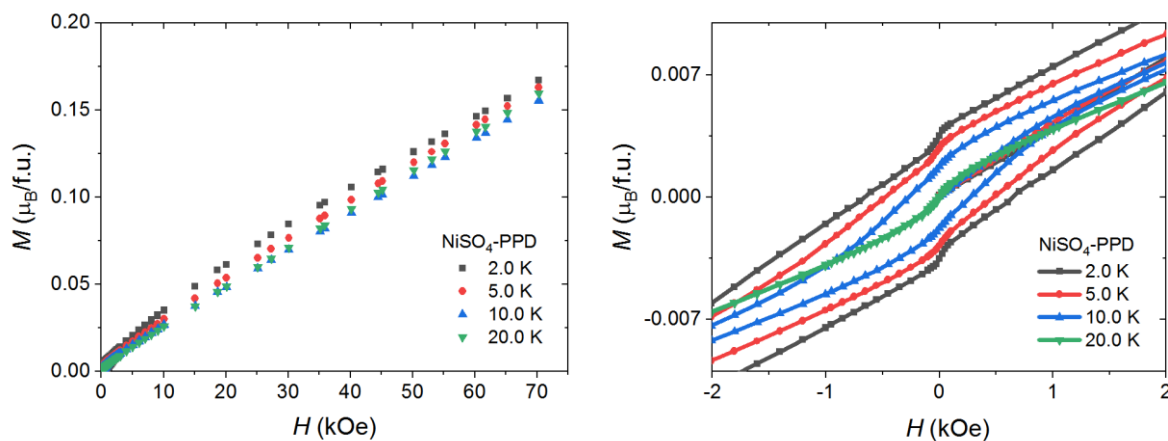


Figure S30. Field dependence of isothermal magnetization for **3** at 2.0 K (black squares), 5.0 K (red circles), 10.0 K (blue triangles) and 20.0 K (green triangles).